Journal of the Korean Chemical Society
2021, *Vol. 65, No. 2*
Printed in the Republic of Korea
https://doi.org/10.5012/jkcs.2021.65.2.93

Transition Metal Complexes Derived From 2-hydroxy-4-(*p*-tolyldiazenyl)benzylidene)-2-(*p*-tolylamino)acetohydrazide Synthesis, Structural Characterization, and Biological Activities

Ahmed N. Alhakimi[†,‡,*], Mohamad M. E. Shakdofa[§,#], S. El-Sayed Saeed[†], Adel M. E. Shakdofa[¶], Maged S. Al-Fakeh[†], Ashwaq M. Abdu[†,$], and Ibrahim A. Alhagri[†,‡]

[†]*Department of Chemistry, College of Science, Qassim University, Buraidah-51452, Saudi Arabia.*
**E-mail: A.Alhakimi@qu.edu.sa*
[‡]*Department of Chemistry, Faculty of Science, Ibb University, Ibb, Yemen.*
[§]*Department of Chemistry, College of Science and Arts, Khulais, University of Jeddah, Saudi Arabia.*
[#]*Inorganic Chemistry Department, National Research Center, P.O. 12622, El-bohouth St., Dokki, Cairo, Egypt.*
[¶]*Department of Chemistry, Faculty of Science, Menoufia University, Shebin El-Kom, Egypt.*
[$]*Key Laboratory of Applied Surface and Colloid Chemistry, MOE/School of Chemistry and Chemical Engineering, Shaanxi Normal University, Xi'an 710062, China.*

(Received December 5, 2020; Accepted January 26, 2021)

ABSTRACT. Mononuclear Cu(II), Ni(II), Co(II), Mn(II), Zn(II), Fe(III), Ru(III) , and UO_2(II) complexes of 2-hydroxy-4-(*p*-tolyldiazenyl)benzylidene)-2-(*p*-tolylamino)acetohydrazide **(H_2L)** were prepared by direct method. The ligand and its complexes were isolated in solid state and characterized by analytical techniques such as elemental and thermal analyses, molar conductance, magnetic susceptibility measurements and spectroscopic techniques such as UV-Visible, IR, ^{1}H-NMR and ^{13}C-NMR. The spectral data indicated that the ligand acted as neutral/monobasic bidentate or monobasic/dibasic tridentate ligand bonded to the metal ions through the oxygen atom of ketonic or enolic carbonyl group, azomethine nitrogen atom and deprotonated/protonated phenolic oxygen atom forming either tetragonally distorted octahedral or octahedral. Antimicrobial activities of the ligand and its complexes were evaluated against *Escherichia coli, Bacillus subtilis* and *Aspergillus niger* by well diffusion method. The results of antifungal activity showed that the Fe(III) complex **(10)** exhibited higher antifungal against *Aspergillus niger* than the other complexes. However, the results of antibacterial activity revealed that Cu(II) complex **(4)** is the most active against *Escherichia coli* while the Cu(II) complex **(5)** and Fe(III) complex **(10)** exhibited higher antibacterial effect on *Bacillus subtilis* than the other complexes.

Key words: Antimicrobial, Azo-Hydrazone, Acetohydrazide, Azo-aldehyde, Metal complexes

INTRODUCTION

Hydrazones are firstly prepared by Emil Fischer in 1884, It is characterized by a structure R_2R_1C=N-N-CR=O.[1] They represent a branch of Schiff base which play an important role in several field as well as It have enormous attention because of its versatility as coordination ligands for the preparation and development of new transition metal complexes. Hydrazones display keto-enol tautomerism and exhibit several modes as neutral, monoanionic or dianionic forms to metal ions with a wide variety of coordination numbers. They form mononuclear, binuclear, trinuclear and tetranuclear metal complexes depending on factors such as additional donor atoms (N or O) in a suitable position for chelation, the nature of the hydrazone ligand, the identity and oxidation state of the metal, the metal-ligand ratio, and the pH of the medium. Hydrazones and their complexes play an important role in various fields such as pharmaceutics, enzyme inhibitors,[2] antioxidant,[3] antibacterial,[4] antidiabetic,[5] antiviral,[6] antifungal,[7] antimicrobial,[8] anti-inflammatory,[9] antituberculosis,[10] anticoagulants,[11] antitumor,[12] anticonvulsant,[11] antiproliferative[13] and antimalarial agents.[14] The addition of azo-linkage (–N=N–) to the skeleton of hydrazone gives it applied capabilities in more fields such as coloring in fibers,[15] photoelectronic,[16] printing materials,[17] optical technology,[18] dyeing in textile,[19] anti-corrosion,[20] and also in biological fields,[21] In addition, the compounds incorporating both hydrazone and azo linkage have been attracted numerous researchers' attention because of their important and effective role in different fields.[13,18b,22] The presence of aryl acetohydrazide moiety linked with the azo systems in their structural lead the ligand also exhibits a wide spectrum of colors and therefore they found to alternate the applications in various fields such as the textile industry,[15] designing of optical storage devices.[23] Both azo compounds and hydrazone are also important compounds in medicinal and biological fields.[22b]

It has been suggested that the azomethine linkage might be responsible for the biological activity achieved by Schiff base.[13,22a,22b,24] Lawrence *et al*. emphasizes the common synthetic routes, several useful applications of hydrazones and azo compounds, as well as their common voltametric properties under oxidative and reductive conditions, with an emphasis on non-aqueous media.[25] Because of the broad applications of the compounds incorporating hydrazone and/or azo linkage, this study directed to synthesize a new azo-hydrazone of named, 2-hydroxy-4-(*p*-tolyldiazenyl)benzylidene)-2-(*p*-tolylamino)acetohydrazide and its mononuclear Cu(II), Ni(II), Co(II), Mn(II), Zn(II), Fe(III), Ru(III), and UO_2(II) complexes. The structure of the prepared compounds was investigated by spectral and analytical techniques such as IR, NMR, and electronic absorption spectra as well as elemental and thermal analyses in addition to the magnetic and molar conductance measurements for complexes. The work was extended to investigate the in-vitro bactericidal and fungicidal activities of the prepared compounds toward bacterial strains *Escherichia coli* and *Bacillus subtilis* as well as fungal strain *Aspergillus niger* by agar well diffusion method.

EXPERIMENTAL

Chemicals

All used reagents employed for the preparation of the ligand and its complexes were of the analytical grade and used without further purification, 2-hydroxy-4-((4-methylphenyl)diazinyl) benzaldehyde and 2-(*p*-toluidino) acetohydrazide were prepared by published methods.[26] DMSO (assay and absolute ethanol (assay ≥99.8%) were used. Metal salts: $CuCl_2{\cdot}2H_2O$, $Cu(SO_4){\cdot}5H_2O$, $Cu(NO_3)_2{\cdot}3H_2O$, $Cu(CH_3COO)_2{\cdot}H_2O$, $FeCl_3{\cdot}6H_2O$ $Co(CH_3COO)_2{\cdot}4H_2O$, $Zn(CH_3COO)_2{\cdot}2H_2O$, $Mn(CH_3COO)_2{\cdot}4H_2O$, and $Ni(CH_3COO)_2{\cdot}4H_2O$ were provided from SIGMA-ALDRICH company. $RuCl_3{\cdot}3H_2O$, $UO_2(CH_3COO)_2{\cdot}2H_2O$, were provided from American-Elements. TLC confirmed the purity of all prepared compounds.

Physical Measurements

The elemental analysis (C, H, N) of prepared compounds were analyzed in the Micro-Analytical Laboratory, Cairo University, Egypt. The metal and chloride ions content were analyzed by Standard analytical methods.[27] IR spectra of the acetohydrazide and its metal complexes were measured in the 400-4000 cm^{-1} range with KBr discs technique on Perkin–Elmer 1430 infrared spectrophotometer. The Electronic absorption spectra in the 200-800 nm regions were recorded using 1-cm quartz cells using DMSO as a solvent. on a on UV-6100PCS double-beam spectrometer. The JEOL EX-400 MHz FT-NMR spectrometer was used to measure the NMR spectra in deuterated dimethyl sulfoxide (DMSO-d_6) as a solvent. The Shimadzu DT-30 thermal analyzer was used to carry out the thermal analysis (TG) from room temperature to 800 °C at a heating rate of 10 °C/min. Gouy Matthey Balance was used to measure the magnetic susceptibilities at 25 °C and were calculated by published equation.[28] Diamagnetic corrections were estimated from Pascal's constant.[29] Tacussel type CD6NG conductivity bridge was used to record the molar conductivity of 10^{-3} M solutions (DMF). The resistance measured in ohms and the molar conductivities were calculated by published equation.[30]

Synthesis of the ligand, 2-hydroxy-4-(*p*-tolyldiazenyl)-benzylidene)-2-(*p*-tolylamino)acetohydrazide (H_2L) (1)

The azo hydrazone **(1)**, 2-hydroxy-4-(*p*-tolyldiazenyl)benzylidene)-2-(*p*-tolylamino) acetohydrazide (H_2L) **(1)** was prepared by adding the ethanolic solution of 2-hydroxy-4-((4-methylphenyl) diazinyl) benzaldehyde (240 mg, 1 mmol in 20 mL) to ethanolic solution of 2-(*p*-toluidino)acetohydrazide (179 mg, 1 mmol, in 20 mL). The mixture was refluxed while stirring for one hour. The formed solid product was filtered, washed with cold ethanol, followed by crystallization from ethanol. Finally dried under vacuum over anhydrous $CaCl_2$ (*Scheme* 1). The formed ligand **(1)** $C_{23}H_{23}N_5O_2$ (FW = 401.19), yield; 90%, color; dark red. Elemental Anal. Calcd. % C, 68.81; H, 5.77; N, 17.44. Found% C, 69.09; H, 5.48; N, 17.66. FTIR (KBr, cm^{-1}); 3415(w) υ(OH), 3358 υ(^{7}NH), 3251 (^{11}NH), 1690 υ(^{9}C=O), 1615 υ(^{13}C=N), 1483, υ(N=N), 1257 υ(^{15}C-OH), 970 υ(N-N) cm^{-1}. ^{1}H-NMR (DMSO-d_6, 400 MHz): δ = 11.23 (s, 1H, OH), 10.27 (s, H, ^{11}NH), 7.87 (s, 1H, ^{7}NH), 8.34 (s, 1H, N=C-H), 6.43-8.19 ppm (m, 11 H, aromatic protons) δ = 2.29 (s, 6H, $^{29\&30}CH_3$), δ = 4.11 (s, 2H, $^{8}CH_2$). ^{13}C-NMR (DMSO-d6, 90 MHz): δ = 169.6 (C=O), δ = 165.1 (C-OH), δ = 150.2 (^{17}C-N=N), δ = 147.2 (^{23}C-N=N), δ = 145.1 (C=N), δ = 141.1 (^{1}C-NH), δ = 111.4-139.1 (aromatic carbon), δ = 50.3 ppm ($^{8}CH_2$), δ = 21.3 ppm ($^{29}CH_3$) δ = 20.6 ppm ($^{30}CH_3$).

Preparation of the Metal Complexes

The metal complexes **(2-3)** and **(5-11)** were prepared by mixing a hot ethanolic solution of the metal salts: $CuCl_2{\cdot}2H_2O$, $Cu(NO_3)_2{\cdot}3H_2O$, $Cu(CH_3COO)_2{\cdot}H_2O$, $Cu(SO_4){\cdot}5H_2O$ $Co(CH_3COO)_2{\cdot}4H_2O$, $Mn(CH_3COO)_2{\cdot}4H_2O$, $Ni(CH_3COO)_2{\cdot}4H_2O$ $Zn(CH_3COO)_2{\cdot}2H_2O$, $FeCl_3{\cdot}6H_2O$ or $RuCl_3{\cdot}3H_2O$ (1 mmol, in 30 mL of ethanol) with a suitable amount of a hot ethanolic solution of the ligand **(1)** (401 mg 1 mmol, 30 mL ethanol). The mixture was then refluxed for 3 hours.

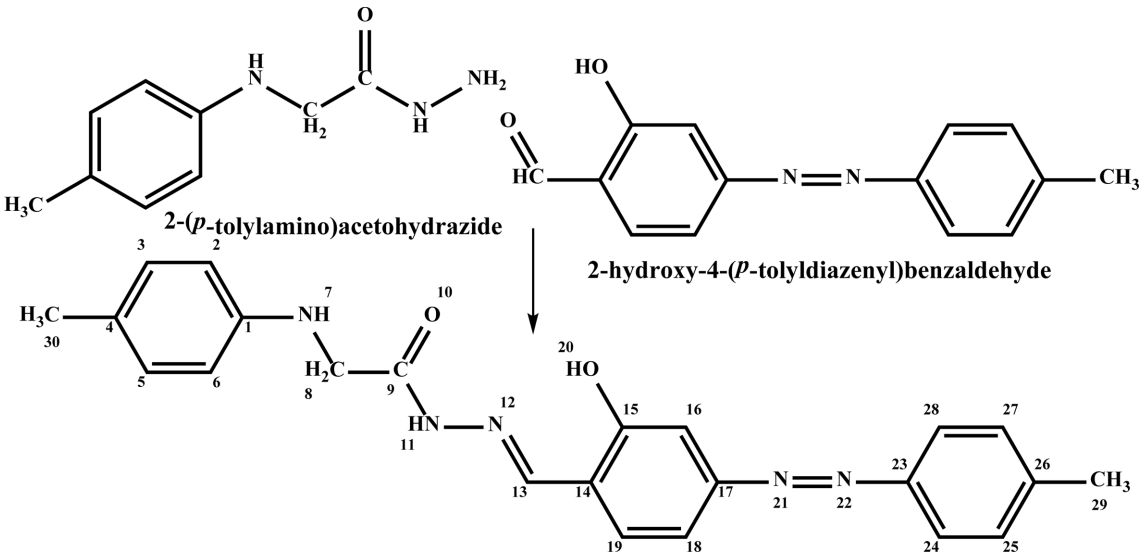

***Scheme* 1.** Preparation of the ligand, 2-hydroxy-4-(*p*-tolyldiazenyl)benzylidene)-2-(*p*-tolylamino)acetohydrazide.

The formed precipitates were filtered, washed with ethanol, then with diethyl ether and dried under vacuum over anhydrous $CaCl_2$. The Cu(II) and UO_2(II) complexes **(4)** and **(12)** were prepared by mixing a hot ethanolic solution of the metal acetate: $Cu(CH_3COO)_2 \cdot H_2O$ or $UO_2(CH_3COO)_2$ (1 mmol, in 30 mL of ethanol) with a suitable amount of a hot ethanolic solution of the ligand **(1)** (801 mg, 2 mmol, 30 mL ethanol). The mixture was then refluxed for 3 hours. The formed precipitates were filtered, washed with ethanol, then with diethyl ether and dried under vacuum over anhydrous $CaCl_2$. The physical properties, elemental analysis and the spectroscopic data of the prepared complexes as shown as follow:

Copper(II) complex (2): $[Cu(HL)Cl(H_2O)_2]$. $C_{23}H_{26}CuN_5O_4Cl$ (FW = 535.49), yield; 85%, M.P.>300; color; green, molar conductance (Λ) = 12.4 $\Omega^{-1}cm^2mol^{-1}$. Elemental Anal. Calcd. %; C, 51.59, H, 4.89; N, 13.08 Cu, 14.86; (Found) % C, 51.88, H, 4.78; N, 13.39; Cu, 14.57. FTIR (KBr, cm^{-1}), $\upsilon(H_2O)$, 3420(br) $\upsilon(^7NH)$, 3358(br) $\upsilon(^{11}NH)$, 3251 υ(NH), 1669 $\upsilon(^9C{=}O)$, 1608 $\upsilon(^{13}C{=}N)$, 1465 υ(N=N), 1312 $\upsilon(^{15}C\text{-}O)_{ph}$, 1014 υ(N-N), 592 υ(Cu-O), 508 υ(Cu←O), 475 υ(Cu←N).

Copper(II) complex (3): $[Cu(HL)(NO_3)(H_2O)_2]$ $C_{23}H_{26}CuN_6O_7$ (FW = 562.04), yield; 75%, M.P. >300. Its color is olive and Λ = 15.1 $\Omega^{-1}cm^2mol^{-1}$. Elemental Anal. Calcd. %; C, 49.15; H, 4.66; N, 14.95; Cu, 14.15. Found %: C, 49.32; H, 4.82; N, 14.65; Cu, 14.00. FTIR (KBr, cm^{-1}); 3420(br) $\upsilon(H_2O/OH)$, 3298 $\upsilon(^7NH)$, 1609 υ(C=N), 1539, 1306 υ(N=C-O), 1466 υ(N=N), 1253 $\upsilon(^{15}C\text{-}OH)$, 1036 υ(N-N), 593 υ(Cu-O), 512 υ(Cu←O), 475 υ(Cu←N), 1422, 1383 cm^{-1} (Δ=39) $\upsilon(NO_3)$.

Copper(II) complex (4); $[Cu(H_2L)_2(CH_3COO)_2]$, $C_{50}H_{52}CuN_{10}O_8$ (FW = 984.57), yield; 77%, melting points (M.P.) >300. Its color is brown, Λ = 15.3 $\Omega^{-1}cm^2mol^{-1}$. Elemental Anal. Calcd. %; C, 61.22; H, 5.58; N, 15.52, Cu, 8.08. Found%; C, 60.99; H, 5.45; N, 15.25 Cu, 7.78. FTIR (KBr, cm^{-1}); 3430 υ(OH): 3363, 3261, υ(NH), 1693 υ(C=O), 1610 (C=N), 1474 υ(N=N), 1257 $\upsilon(^{15}C\text{-}OH)$, 995 υ(N-N), 500 υ(Cu←O), 465 υ(Cu←N), 1562,1376 cm^{-1} (Δ=186) $\upsilon_{sy}CH_3COO$, $\upsilon_{asy}CH_3COO$.

Copper(II) complex (5); $[Cu(L)(H_2O)_3]$, $C_{23}H_{27}CuN_5O_5$ (FW = 517.05), yield; 72%, M.P.>300. Its Color is olive and Λ = 11.9 $\Omega^{-1}cm^2mol^{-1}$. Elemental Anal. Calcd. %; C, 53.43; H, 5.26; N, 13.55; Cu, 14.45; Found %; C, 53.60.; H, 5.49; N, 13.25; Cu, 14.09. FTIR (KBr, cm^{-1}); 4450(br) $\upsilon(H_2O)$, 3388 (^{7}NH), 1604 υ(C=N), 1537, 1373 υ(N=C-O), 1465 υ(N=N), 1308 $\upsilon(C\text{-}O)_{ph}$, 1014 υ(N-N), 594, 510 υ (Cu-O), 475 υ(Cu←N).

Cobalt(II) complex (6); $[Co(HL)(CH_3COO)(H_2O)_2]$, $C_{25}H_{29}CoN_5O_6$ (FW = 554.47), yield; 63%, M.P.>300. Color is reddish brown, Λ = 10.2 $\Omega^{-1}cm^2mol^{-1}$. Elemental Anal. Calcd. %; C, 54.16; H, 5.27; N, 12.63; Co, 13.51; Found % C, 54.39.; H, 5.50; N, 12.88; Co, 13.65; FTIR (KBr, cm^{-1}); 3435(br) $\upsilon(H_2O)$, 3294 υ(NH), 1604 υ(C=N), 1525, 1314 υ(N=C-O), 1254 $\upsilon(^{15}C\text{-}OH)$, 1038 υ(N-N), 594 υ(Co-O), 511 υ(Co←O), 473 υ(Co←N), 1542, 1371 (Δ=171) $\upsilon_{sy}CH_3COO$, $\upsilon_{asy}CH_3COO$.

Manganese(II) complex (7); $[Mn(HL)(CH_3COO)(H_2O)_2]$ $C_{25}H_{29}MnN_5O_6$ (FW = 550.47), yield; 77%, M.P.>300. Color is dark yellow and Λ = 9.6 $\Omega^{-1}cm^2mol^{-1}$. Elemental Anal.

Calcd. %; C, 54.55; H, 5.31; N, 12.72; Mn, 13.57; Found: C, 54.52.; H, 5.56; N, 12.44; Mn, 13.18; FTIR (KBr, cm^{-1}); 3445 (br) υ(H_2O/OH), 3388 υ(NH), 1610 υ(C=N), 1590 υ(N=C-O), 1465 υ(N=N), 1315 υ(N=C-O), 1250 υ(^{15}C-OH), 1009 υ(N-N), 580 υ(Mn-O), 506 υ(Mn←O), 487 υ(Mn←N), 1540, 1340 cm^{-1} (Δ=200) $\upsilon_{sy}CH_3COO$, $\upsilon_{asy}CH_3COO$.

Zinc(II) complex (8); [Zn(HL)(CH_3COO)(H_2O)$_2$], $C_{25}H_{29}ZnN_5O_6$ (FW = 560.92),yield; 58%, M.P.>300. Color is pale yellow; Λ = 11.50 $\Omega^{-1}cm^2\,mol^{-1}$. Elemental Anal. Calcd. %; C, 53.53; H, 5.21; N, 12.49; Zn, 14.51; Found %; C, 53.30.; H, 5.30; N, 12.41; Zn, 14.09. FTIR (KBr, cm^{-1}); 3430(br) υ(H_2O/OH), 3284 υ(NH), 1600 υ(C=N), 1585 υ (N=C-O), 1490 υ(N=N), 1300 υ(N=C-O), 1253 υ(^{15}C-OH), 1013 υ(N-N), 582 υ(Zn-O), 532 υ(Zn←O), 458 υ(Zn←N), 1545, 1335 cm^{-1} (Δ=210) $\upsilon_{sy}CH_3COO$, $\upsilon_{asy}CH_3COO$. ^{1}H-NMR (DMSO-d_6, 400 MHz): δ = 11.94 (s, 1H, OH), 8.34 (s, 1H, ^{7}NH), 8.91 (s, 1H, N=C-H), 6.59-8.15 ppm (m, 11 H, aromatic protons) δ = 2.33 (s, 6H, $^{29\$30}CH_3$), δ = 4.27 (s, 2H, $^8CH_2$), δ =1.55 (s, 3H,CH_3COO); ^{13}C-NMR (DMSO-d_6, 90 MHz): δ = 167.1(C=O), δ =160.4(C-OH), δ =150.1 (^{17}C-N=N), δ =147.6 (^{23}C-N=N), δ = 142.3 (C=N), δ =141.0 (^{1}C-NH), δ = 111.9-130.4 (aromatic carbon), δ = 48.8 ppm ($^8CH_2$), δ = 23.4 ppm ($^{29}CH_3$) δ = 21.7 ppm ($^{30}CH_3$), δ = 172.3, 14.4(CH_3COO).

Nickel complex (9); [Ni(HL)(OAc)(H_2O)$_2$] $C_{25}H_{29}NiN_5O_6$ (FW = 554.23), yield; 77%, M.P.>300. Color is brown, Λ = 15.3 $\Omega^{-1}cm^2\,mol^{-1}$. Elemental Anal. Calcd. %; C, 54.18; H, 5.27; N, 12.64; Ni, 13.48; Found % C, 54.12.; H, 4.97; N, 12.55; Ni, 13.16. FTIR (KBr, cm^{-1}); 3435(br) υ(H_2O/OH), 3287 υ(NH), 1604 υ(C=N), 1588 ν(N=C-O), 1465 ν(N=N), 1321 υ(N=C-O), 1249 υ(^{15}C-OH), 1018 υ(N-N), 566 (Ni-O), 506 υ(Ni←O), 489 υ(Ni←N), 1556, 1346 cm^{-1} (Δ=210) $\upsilon_{sy}CH_3COO$, $\upsilon_{asy}CH_3COO$.

Iron(III) complex (10); [Fe(L)Cl(H_2O)$_2$] $C_{23}H_{25}FeClN_5O_4$ (FW = 526.78), Yield: 65%, M.P.>300. Its color is dark brown and Λ = 16.5 $\Omega^{-1}cm^2\,mol^{-1}$. Elemental Anal. Calcd. % C; 52.44; H, 4.78; N, 13.29, Cl, 6.73, Fe, 15.16. Found %; C, 52.67; H, 4.77; N, 13.50, Cl, 6.33, Fe, 15.20. FTIR (KBr, cm^{-1}); 3435 υ(H_2O), 3360 υ(NH), 1608 υ(C=N), 1531, 1370 υ(N=C-O), 1466 υ(N=N), 1317 υ(C-O)$_{ph}$, 999 υ(N-N), 567 υ(Fe-O), 507 υ(Fe←N).

Ruthenium(III) complex (11); [Ru(HL)Cl_2(H_2O)]·2H_2O, $C_{23}H_{28}RuCl_2N_5O_5$ (FW = 626.07), yield; 73%, M.P.>300. Its color is dark brown and Λ = 17.5 $\Omega^{-1}cm^2\,mol^{-1}$. Elemental Anal. Calcd. %; C, 44.01; H, 4.51; N, 11.18; Cl, 11.32; Ru, 19.98; Found % C, 44.22.; H, 4.26; N, 11.29; Cl, 11.00; Ru, 19.83. FTIR (KBr, cm^{-1}); 3440 υ(H_2O), 3358, 3251 υ(NH), 1680 υ(C=O), 1583 υ(C=N), 1485 υ(N=N), 1280 υ(C-O)$_{ph}$, 970 υ(N-N), 562 υ(Ru←O), 513 υ(Ru←O), 480 υ(Ru←N).

Uranium (VI) complex (12); [UO_2(HL)$_2$(H_2O)$_2$] $C_{49}H_{48}UO_2N_{10}O_6$ (FW = 1106.93), yield 65%, and M.P.>300. Color is orange; Λ = 10.5 $\Omega^{-1}cm^2\,mol^{-1}$. Elemental Anal. Calcd. %; C, 49.91; H, 4.33; N, 12.65, U, 25.84; Found % C, 49.38.; H, 4.52; N, 12.97, U, 25.43. FTIR (KBr, cm^{-1}); 3400(br), υ(H_2O/OH), 3300(w) υ(NH), 1614 υ(C=N), 1547, 1375 υ(N=C-O), 1470, υ(N=N), 1318 υ(C-O)$_{ph}$, 1015 υ(N-N), 956 υ(O=U=O), 512 υ(U-O), 472 cm^{-1} υ(U←N).

In-vitro Antimicrobial Activity

The assessment of the antimicrobial activities of all compounds **(1-8)** were tested against different strains of Gram-Positive and Gram-negative bacteria as well as fungal strains by agar well diffusion method.[31] The tested strains were *Escherichia coli (E. coli), Bacillus subtilis (B. subtilis*) and, *Aspergillus niger (A. niger)*. The bacteria and filamentous fungi were cultured on Mueller-Hinton agar medium and Czapek Dox's agar (CDA) medium, respectively at pH 7.4. The agar plates were incubated at 37 °C for 24 h (bacteria) and at 28 °C for 4 days (fungi). Tetracycline (Sigma, USA) was used for the bacteria while amphotericin B (Sigma, USA) was used for the fungi. A negative control (DMSO; 2% v/v) was also included to compare the activity. The appearance of zones of inhibition was regarded as positive for the presence of antimicrobial action in the test substance. Subsequently, each value was the average of three independent replicates and the activity index for the complexes was calculated by following formula.[32]

$$\text{Activity index} = \frac{\text{Diameter of inhibation zone by test compound}}{\text{Diameter of inhibation zone by standard}} \times 100$$

RESULTS AND DISCUSSION

The reaction of 2-(*p*-toludino) acetohydrazide with 2-hydroxy-4-((4-methylphenyl) diazinyl) benzaldehyde in 1:1 mole ratio led to the formation of ligand **(H_2L,1)**, as shown in *Scheme* 1. The reaction of the ligand **(1)** with metal salts using (1:1) molar ratio, it gives complexes; **(2-3)**, and **(5-11)** while complexes **(4)** and **(12)** was prepared in molar ratio 1M:2L. All prepared compounds are intensely colored, crystalline solids, stable at room temperature and do not decompose after prolonged storage. The complexes are insoluble in water, ethanol, methanol, benzene, toluene acetonitrile, and chloroform, but completely soluble in dimethylformamide (DMF) or dimethyl sulfoxide (DMSO). The molar conductivity values of synthesized metal complexes are in the

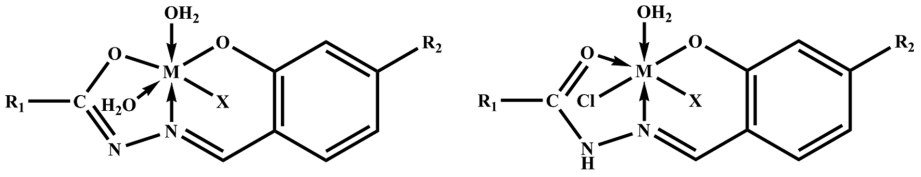

M= Cu(II), X= H_2O (5)
M= Fe(III), X= Cl (10)
R_1 =$C_8H_{10}N$, R_2 = $C_7H_7N_2$

M= Cu(II), X= H_2O (2)
M= Ru(III), X= Cl (11)
R_1 =$C_8H_{10}N$, R_2 = $C_7H_7N_2$

***Figure* 1.** The structure representation of Cu(II), Fe(III), Ru(III) complexes.

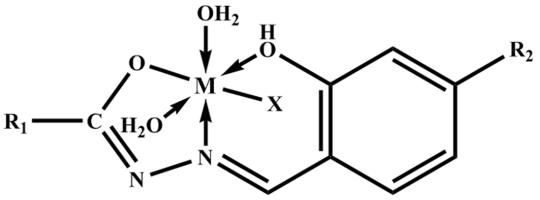

$[M(HL)X(H_2O)_2]$
M= Cu(II), X= NO_3 (3)
M= Co(II), X= OAc (6)
M= Mn(II), X= OAc (7)
M= Zn(II), X= OAc (8)
M= Ni(II), X= OAc (9)
R_1 =$C_8H_{10}N$, R_2 = $C_7H_7N_2$

***Figure* 2.** The structure representation of Cu(II), Co(II), Mn(II), Zn(II) and Ni(II) complexes.

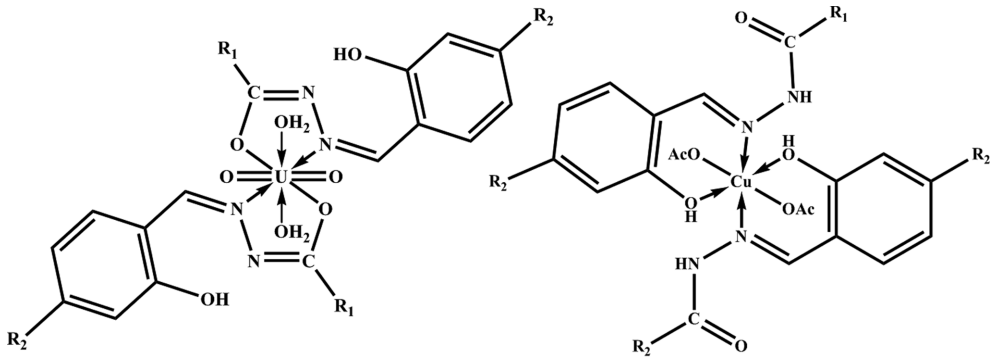

$UO_2(HL)_2(H_2O)_2]$ (12)
R_1 =$C_8H_{10}N$, R_2 = $C_7H_7N_2$

$[Cu(H_2L)_2OAc_2]$ (4)
R_1 =$C_8H_{10}N$, R_2 = $C_7H_7N_2$

***Figure* 3.** The structure representation of Cu(II), and UO_2(II) complexes.

6.6–25.5 $\Omega^{-1}cm^2mol^{-1}$ range indicating their non-electrolytic nature.[33] Analytical and spectral data are compatible with the suggested structures as shown in *Figs*. 1-3. The elemental analyses confirmed that the complexes **(2-3)**, **(5-10)** and **(11)** were composed in molar ratio 1 Ligand:1 Metal, whereas the complexes **(4)** and **(12)** were found to be formed in molar ratio 2 L : 1 M. Many attempts were made to grow single crystal but unfortunately, they failed.

^{1}H- and ^{13}C-NMR Spectra of Ligand

The ^{1}H-NMR spectrum of the ligand in DMSO-d^6 as a solvent (*Supp*. 1) showed signals, which are consistent with the proposed structure. The spectrum of the ligand showed the absence of the signal of the amino group ($-NH_2$) characteristic to the starting material (hydrazide). The spectrum showed several signals, the chemical shifts observed as a singlet at 11.23 (s, 1H), 10.27 (s, H), 7.87 (s, 1H), 8.34 may be assigned to the protons of the hydroxyl (OH) (^{11}NH), and (^{7}NH) respectively.[34] The appearing of these proton resonances at high δ values could be due to their connection to extremely electronegative atoms oxygen and nitrogen. This assignment was assured by considerably decreasing intensity of these bands in the deuterated spectra. The situation of these signal in the downfield region indicates the probability of hydrogen bonding formation by these hydrogen atoms.[35] The azomethine proton (H-C=N) was appeared at 8.34 ppm.[34b,35–36] This assignment confirmed by the deuterated spectra in which the intensity of these bands is considerably decreased. The multiples which were appeared in the 6.47–8.46 (m, 11H) ppm range, may be attributed to the aromatic protons. It was clear from the ^{1}H-NMR spectrum of the ligand that it exhibits the keto

form only and no evidence for the presence of the enol form. This result was confirmed from the appearance of the signal of the (NH) and phenolic (OH) only and the absence of the (OH) signal of the enolic form which was reported by many authors.[34b] The ^{1}H NMR spectrum of Zn(II) complex **(8)** verified that the proton of amide group CO-NH is missed denoting to the bonding of the ligand (H_2L) with the Zn(II) ion in its enolic form. while phenolic protons shifted to low field at δ = 11.84 ppm, which could be due to intramolecular hydrogen bonding with the carbonyl group, since the carbonyl group is chelated with the metal ion. On the other hand, the significant downfield shift of the azomethine (8.91 ppm) and phenolic (11.94 ppm) protons signals in the complex relative to the corresponding free ligand confirmed the coordination of the azomethine nitrogen and phenolic oxygen atoms to the Zn(II) ion. Aromatic protons appeared in the δ = 6.59-8.15 ppm range and the singlet for methyl groups appeared at δ = 2.33 ppm. While the singlet which appeared at 1.55 ppm could be assigned to the proton of acetate group.[37] The ^{13}C-NMR spectrum of the ligand (*Supp*. 3) showed signal at 169.1 ppm which could be assigned to carbon atom of the carbonyl group (^{9}C=O) while the chemical shift which observed at 165.1 ppm assigned to the carbon atom attached to a hydroxyl group (^{15}C-OH).[35–36,38] While the chemical shifts of the carbons C^{16}, C^{18}, C^{24}, C^{26}, (δ = 111.3, 116.7, 123.9, 124.3 ppm) are typical values of N=N group connected to C^{17} (δ = 150.2 ppm) and C^{23} (δ = 147.2 ppm).[39] The chemical shift appeared at 145.1, 141.1 ppm were assignable to the azomethine carbon (^{13}C=N) and the aromatic carbon attached to amine group (^{1}C-NH).[35–36,38a] However, the peaks observed in the 113.4-139.1 ppm range were assigned to the other aromatic carbons.[38a] The chemical shift appeared at 50.3, 21.3 and 20.5 ppm could be belonging to the proton's methylene –CH_2-N and methyl groups, respectively.[40] In the ^{13}CNMR spectrum of Zn(II) complex (*Supp*. 4), the carbon atoms of carbonyl, phenolic and azomethine signals shifted to up-field by about 2.5-4.7 ppm in comparing with the parent ligand. This up-field shift may be due to the movement of electron density from carbonyl δ(C=O) and azomethine linkages to the Zn(II) ion upon chelation that could have caused the carbon nuclei to be de-shielded because of the up-field shifts.[41] In addition, this spectrum also shows two signal at 172.4 and 14.4 ppm which was referred to the carbon atoms of acetate group.[37]

FTIR Spectra

The bonding mode of the ligand in the metal complexes has been deduced from their IR spectra. The important spectral bands of the ligand and its metal complexes are presented in the experimental part. The spectrum of the ligand (*Supp*. 5) showed a medium band at 3251 cm^{-1} which may be assigned to the ν(^{11}NH) group, whereas the strong band at 1690 cm^{-1} due to the carbonyl group of the hydrazide moiety.[34c] This observation indicates that the ligand is present in the ketonic form in the solid-state.[42] The spectrum showed a sharp band in the 3415 cm^{-1}, which may be assigned to the stretching vibration of the phenolic hydroxyl group.[34c] The relatively strong and medium bands, which located at 3358, 1615, 1483 and 970 cm^{-1} corresponded to the amine groups (^{7}NH), azomethine,[43] azo,[44] and ν(N-N) groups[42] respectively. The band, which appeared at 1257 cm^{-1} is due to the ν(C-OH) of the phenolic moiety.[42] The bonding of the ligand can be predicted by comparison the IR spectra of the complexes (*Supp* 6-12) with that of the free ligand. The IR spectra data obtained for complexes showed that the ligand **(H_2L)** behaves as either of the following evidence:

1) Neutral bidentate as in case of complex **(4)** in which the ligand coordinated to metal ions via protonated hydroxyl group and the azomethine nitrogen atom. This mode of coordination can be suggested by the following evidence: i) The bands characteristic to υ(^{11}NH) and carbonyl groups were still present in the same position indicating that the carbonyl group did not take part in the coordination. ii) The bands characteristic to the azomethine and hydroxyl groups were shifted and appeared as week band. At the same time, the band due to υ(N-N) was shifted to a higher frequency. This shift refers to the increase in the double bond character is off-setting the loss of electron density via electron donation to the metal ions and further confirmation of the coordination of the ligand via the azomethine and hydroxyl groups.[43]

2) Monobasic bidentate as in complex **(12)** in which the ligand bonded to the metal ions through the enolic carbonyl oxygen (C-O), and azomethine nitrogen (C=N) atoms. This bonding behavior was confirmed by: (i) the bands characteristic to the carbonyl ν(C=O), and ν(NH) groups vanished referring that the ligand bonded in its enolic form via enolic carbonyl oxygen, which is further assured by the occurrence of new peaks in the 1547, 1375 cm^{-1} attributing to the ν(N=C-O) and ν(C-O), respectively.[45] (ii) The characterized frequency of the azomethine group lowered whereas the characterized frequency of ν(N-N) increases and appearing at 1014 cm^{-1}. The increment in the frequency of ν(N-N) band is an obvious reference to the increasing in the double bond property is off-setting the lack of electron density via electron donation to the metal ions and further confirmed that the azomethine group participate in the chelation pro-

cess.[43]

3) Monobasic tridentate as in complexes **(3)** and **(6-9)** in which the ligand bonded to the metal ions through the enolic carbonyl oxygen (C-O), protonated hydroxyl group and azomethine nitrogen atom (C=N).This bonding behavior was confirmed by: i) The band characteristic to the carbonyl υ(C=O), and υ(^{11}NH) groups disappeared indicating that the ligand **(1)** bonded to the metal ions in its enolic form via enolic carbonyl oxygen atom, which is further supported by the appearance of new bands in the 1525-1595 and 1300-1321 cm^{-1} ranges corresponding to the υ(N=^{9}C-O) and υ(^{9}C-O), respectively.[45] ii) The characteristic bands of azomethine and hydroxyl groups band υ(C=N) shifted or appeared as a week band in 1600-1610 and 1247-1257 cm^{-1}. At the same time, the band due to υ(N-N) was shifted to a higher frequency and appeared in 1009-1038 cm^{-1} range. This shift refers to the increase in the double bond character is off-setting the loss of electron density via electron donation to the metal ions and further confirmation of the coordination of the ligand via the azomethine group.[43]

4) Dibasic tridentate as in complex **(5)** and **(10)** in which the ligand **(1)** bonded to the copper and ferric ions through the enolic carbonyl oxygen (C-O), deprotonated hydroxyl oxygen and azomethine nitrogen atoms. This bonding behaviour was supported by the next evidences: i) the bands characteristic to the carbonyl and ν(^{11}NH) groups vanished referring that, the ligand **(1)** bonded via its enolic carbonyl oxygen atom, which is furthermore confirming by the occurrence of new bands at 1537, 1531; 1373, 1370 cm^{-1} referring to the ν(N=^{9}C-O), and ν(^{9}C-O), respectively.[45] (ii) The band characteristic to ν(C=N) group lowered to 1604 and 1608 respectively where the peak belongs ν(N-N) shifted to a higher frequency and appearing at 1014, 999 cm^{-1}. The increment in the frequency of ν(N-N) bond is an obvious reference to the increasing in the double bond property is off-setting the lack of electron density via electron donation to the metal ions and further confirmed that the azomethine group takes part in the chelation.[43] (iii) The shifting in the peak characteristic to phenolic hydroxy group and disappearing of the peak assigned to hydroxyl proton indicating that the deprotonated phenolic oxygen atom participates in the bonding. The appearance of new bands in the 507-594, 500-532 and 458-507 cm^{-1} ranges for the prepared complexes may be assigned to υ(M—O), υ(M←O) υ(M←N). Also, appearance of new bands in 458–513 cm^{-1} range may be assigned to υ(M←N) respectively. These peaks confirm that linkage between ligand and metal ions occurred via oxygen atoms of the enolic/ketonic, protonated/deprotonated phenolic hydroxyl groups as well as azomethine nitrogen atom.[44–46] The nitrate complex **(3)** spectrum showed two peaks at (ν_5)1466 and (ν_1) 1373 cm^{-1}, related to the asymmetric stretch of C_{2v} symmetry, coordinated NO_3 group. The difference between these two peaks (ν_5-ν_1) was used to recognize the covlency degrees of the nitrate group chelation. This difference (Δν) rises as the chelation of the nitrate group changes for monodentate to bidentate and/or bridging manner. Complex **(3)** showed (Δν) value equal to 39 cm^{-1} which is a typical value for a unidentate nitrates bonding. In acetate complexes, the acetate ion may be coordinate to the metal ion in unidentate, bidentate or bridging bidentate behavior.[47] The $\nu_{as}(CO_2)$ and $\nu_s(CO_2)$ of the free acetate ion is ca. 1560 and 1416 cm^{-1}, respectively. In unidentate acetate complexes ν(C=O) is higher than $\nu_s(CO_2)$ and ν(C-O) is lower than $\nu_{as}(CO_2)$. As a consequence, the isolation between the two ν(CO) is higher in unidentate than in free ion but in bidentate the isolation is lower than in the free ion whilst in bridging bidentate the two n(CO) is closer to the free ion.[47b] In complexes **(4)** and **(6-9)** the presence of two new peaks in the 1540-1562 and 1335-1376 cm^{-1} ranges are imputed to the symmetric and asymmetric stretching vibration of the acetate group. The coordination mode of acetate group was deduced from the value of the observed separation (Δ) between the ν_{asy}(COO) and ν_{sy}(COO). The (Δ) values between ν_{asy}(COO) and ν_{sy}(COO) in **(4)** and **(6-9)** complexes were in the 171-210 cm^{-1} range supporting the coordination of acetate group in a monodentate fashion.[47b,47c,48] The IR spectrum of the UO_2)II) complex showed a peak at 956 cm^{-1} which could be imputed to ν(O=U=O).[49]

Magnetic Moment

The magnetic moments of the **(2-7)** and **(9-11)** complexes were measured at room temperature and were presented in *Table* 1. The values of magnetic moment indicating that these complexes are paramagnetic. The copper(II) complexes **(2-5)** showed values in the 1.70-1.80 Bohr Magnetons (B M) range, which are appropriate with one unpaired electron system in octahedral environment.[34b] Cobalt(II) complex **(6)** shows value 4.33 indicating a low spin cobalt(II) complex.[50] Nickel(II) complex **(9)** shows the value of 3.2 BM, which is consistent with two unpaired electrons system of the octahedral nickel(II) complex.[51] The magnetic moment values of manganese(II) **(7)** and iron(III) **(10)** complexes are 5.88 and 5.90 BM, respectively. This suggests octahedral geometry around the manganese(II) and octahedral iron(III) complexes.[52] The magnetic moment value of the ruthenium(III) complex **(11)** is 1.71 BM, which is characteristic of d^5 low spin ruthenium(III) complex.[45,50]

Electronic Spectra

The electronic absorption spectral data of the ligand **(1)** and its metal complexes in DMF solutions (*Supp*. 13) are localized in *Table* 1. The structure of the ligand revealed that, the two lone pairs of electrons for the azo group is not the only interacting non-bonding electrons, since the hydrazone moiety of the ligand contains carbonyl and azomethine which represents an extra source of lone pair of electrons. Thus other ν→π* transitions is expected to take place from these non-bonding orbitals to different molecular orbital extending over such a large molecules.[53] The data revealed that, the ligand comprised three sets of peaks in the UV and visible regions. The first set of the shortest wavelengths appeared at 261 and 295 nm may be assigned to the π→π* transitions in the intra ligand and benzenoid moiety.[34b,38a] The second set observed at 321 and 360 nm may be assigned to n→π* transitions of the azomethine and carbonyl groups.[34b,38a] The third set comprise of two bands: the first one located at 383 nm, which could be attributed to π→π* transition involving the π electron of the azo group.[53–54] Whereas the second band located in the visible region at 440 nm could be assigned to π→π* transition involving the whole electronic system of the compounds with a considerable charge transfer character arising mainly from the phenolic moiety.[53–54] The spectrum of copper complexes **(2-5)** showed a broad band centered in the 520–670 nm range. The position as well as the broadness of this band indicated that copper(II) complexes have a tetragonally distorted octahedral geometry (*Figs*. 1-3). This broad band consists of three superimposed transitions $^2B_{1g}\rightarrow{}^2E_g$, $^2B_{1g}\rightarrow{}^2A_{1g}$ and $^2B_{1g}\rightarrow{}^2B_{2g}$ transition.[47c,55] The cobalt(II) complex **(6)** showed bands at 500, 555, 850 nm, which could imputed to $(\upsilon_3)^4T_{1g}(F)\rightarrow{}^4T_{2g}(P)$, $(\upsilon_2)^4T_{1g}(F)\rightarrow{}^4A_{2g}(F)$ $(\upsilon_1)^4T_{1g}(F)\rightarrow{}^4T_{2g}(F)$ transitions respectively, referring to high spin cobalt(II) octahedral complex (*Fig.* 2).[45,55b] The υ_2/υ_1 ratio for the complex is 1.44 which is lower than the regular range for octahedral cobalt(II) complexes (1.95–2.48), referring that this Cobalt(II) complex has a distorted octahedral geometry.[56] Manganese(II) complexes **(7)** displays week absorption bands at 460, 490, 555 and 670 nm assigned to $^6A_{1g}\rightarrow{}^4T_{1g}(4G)(\upsilon_1)$, $^6A_{1g}\rightarrow{}^4E_g(4G)(\upsilon_2)$, $^6A_{1g}\rightarrow{}^4E_g(4D)(\upsilon_3)$ and $^6A_{1g}\rightarrow{}^4T_{1g}(4p)(\upsilon_4)$ transitions respectively, which characteristic to manganese(II) in an octahedral geometry (*Fig.* 2).[55b,57] Nickel(II) complex **(9)** exhibits three bands located at 500, 555, 800 nm which may be assigned to $^3A_{2g}(F)\rightarrow{}^3T_{1g}(P)(\upsilon_3)$, $^3A_{2g}(F)\rightarrow{}^3T_{1g}(F)(\upsilon_2)$ and $^3A_{2g}(F)\rightarrow{}^3T_{2g}(F)(\upsilon_1)$ spin allowed transitions, which are characteristic to nickel(II) ion in an octahedral structure (*Fig.* 2).[55b,57–58] The υ_2/υ_1 ratio for the complex is 1.31 which is less than the usual range (1.5-1.75), indicating a distorted octahedral nickel(II) complex.[58a] Iron(III) complex **(10)** revealed two bands at 530 and 650 nm which may be assigned to $^6A_{1g}\rightarrow{}^4T_{2g}$ and $^6A_{1g}\rightarrow{}^4T_1(G)$ transitions. These bands are characteristic of an octahedral iron(III) complex (*Fig*. 1).[55b,59] The ground

***Table* 1.** UV-Vis. spectra of the ligand (H_2L) and its metal complexes

No	Bands in DMF	Electronic transition	μ_{eff} (BM)	Geometry
1	261,295, 321, 360 383, 440	n →π* π →π*	----	---
2	280, 320, 350, 380, 435, 670		1.70	Tetragonally distorted octahedral
3	270, 320, 345, 375, 415, 520	$(\nu_3)\ ^2B_{1g}\rightarrow{}^2Eg$, $(d_{x2-y2}\rightarrow d_{xy})$	1.80	
4	270, 345, 375, 430, 460, 550	$(\nu_2)\ ^2B1g\rightarrow{}^2B_{2g}$ $(d_{x2-y2}\rightarrow d_{yz}\ d_{xz})$	1.78	
5	285, 300, 315, 345, 400, 440, 640	$(\nu_1)\ ^2B_{1g}\rightarrow{}^2A_{1g}$ $(d_{x2-y2}\rightarrow d_{z2})$	1.75	
6	245, 320, 385, 415, 440, 500, 555, 850	$^4T_{1g}(F)\rightarrow{}^4T_{1g}(P)$ $^4T_{1g}(F)\rightarrow{}^4A_{2g}$ $^4T_{1g}(F)\rightarrow{}^4T_{2g}(F)$	4.33	Distorted octahedral
7	280, 345, 375, 430, 460, 490, 555	$(\upsilon_1)^6A_{1g}\rightarrow{}^4T_{1g}(4G)$ $(\upsilon_2)^6A_{1g}\rightarrow{}^4E_g(4G)$ $(\upsilon_3)^6A_{1g}\rightarrow{}^4E_g(4D)$ $(\upsilon_4)^6A_{1g}\rightarrow{}^4T_{1g}(4p)$	5.88	Octahedral
8	257, 270, 336, 366, 395, 420	LMCT	Dia.	--
9	250, 285, 340, 385, 415, 460, 500, 555, 800	$^3A_{2g}(F)\rightarrow{}^3T_{1g}(P)(\upsilon_3)$ $^3A_{2g}(F)\rightarrow{}^3T_{1g}(F)(\upsilon_2)\ ^3A_{2g}(F)\rightarrow{}^3T_{2g}(F)(\upsilon_1)$	3.2	Distorted octahedral
10	255, 298, 326, 373, 390, 433, 480, 530, 650	$^6A_{1g}\rightarrow{}^4T_{2g}$ $^6A_{1g}\rightarrow{}^4T_1(G)$	5.90	Octahedral
11	250, 293, 339, 377, 400, 455, 510, 620	LMCT $^2T_2g\rightarrow{}^2A_2g$	1.71	Octahedral
12	270, 287, 345, 365, 390, 440, 490	LMCT	Dia.	--

state of ruthenium(III) is $^2T_{2g}$ and the first excited doublet levels, in order of increasing energy, are $^2A_{2g}$ and $^2A_{1g}$ which arise from the $t_{2g}^4e_g^1$configuration. However, the electronic absorption spectrum of ruthenium(III) complex **(11)** displayed two bands at 500 and 620 nm. The first band may be due to LMCT transition and the second may be assigned to $^2T_{2g}\rightarrow{}^2A_{2g}$ transition. The band positions are like those observed for other octahedral ruthenium(III) complex (*Fig.* 1).[55b,60] The electronic absorption spectrum of UO_2^{2+} complex **(12)** showed one band at 490 nm which may be acribed to ligand to uranium charge transfer.[61] The diamagnetic complexes zinc(II) **(8)** does not show d-d transitions. The bands observed are due to intra-ligand transitions.

Thermal Analysis

To obtain further information about the thermal stability as well as the nature of water molecules in the complexes structure the TG analysis of complexes **(2)**, **(4-5)** and **(9-11)** were recorded in temperature 25-800 °C range (*Supp*. 14-17). The results of the thermal analysis are shown in *Table* 2. The thermal data revealed that the weight loss of the calculating and proposed formulae is agreeable and referred that the complexes are mostly decomposed in two, three or four stages that can be interpreted as following:

1. Dehydration process as in complex **(11)** which took place in the 22-80 °C range with losing in weight equal to 5.87(5.75)% corresponding to removal of two water molecules (*Table* 2).

2. In the TG of complexes **(2)**, **(5)** and **(9-11)** there is a step occurred in the temperature ranged 95 to 225 °C with losing in weight ranged from to 2.61(2.88) to 11.77(12.07)% may be ascribed to the elimination of one, two or three coordinated water molecules.

3. The removal of anions acetate or chloride from complex **(2)**, **(4)** and **(9-11)** took place in the 120-330 °C which can be confirmed from the percentage weight loss (*Table* 2).

4. The last step is the complete degradation of all complexes through departure of the organic part in the 210-720 °C leaving the metal oxide which can be confirmed from the percentage of weight loss (*Table* 2).

In-vitro Antimicrobial Activity

Well Diffusion Method at 10 mg/mL concentration in DMSO was used to measure the antimicrobial activity against *E. coli, B. subtilis* and *A. niger.* The results (*Table* 3) showed that complex **(12)** is inactive against all used strains while the other synthesized complexes were more active than ligand but less than standard drug with IZ ranged from 11-14 mm and AI ranged from 65-82%. The most active complex was the iron(III) complex (**10**) with 14 mm inhibition zone (AI=82%), and the second was manganese complex **(7)** with 13 mm inhibition zone (AI=76%). The order of antifungal activity is **(10)>(7)>(3)=(9)=(11)>(2)=(6)** > **(1)=(4)=(8)** as shown in *Fig.* 4. In the case of antibacterial activity against *E. coli,* the complex **(3)** is inactive, while the ligand and other complexes showed low activity in comparison with Tetracycline as an antibacterial standard drug. The order of antibacterial activity against *E. coli* is **(7)> (10)>(5)>(6)=(9)>(11)>(2)=(4)>(Ligand)=(8)** as shown in *Fig*. 4. While in the case of antibacterial activity against

***Table* 2.** The thermal analysis (TG) of some complexes

No.	Temp. range (°C)	Weight Loss (%) Found (calcd.)	Assignment	Composition of the residue
(2)	105-170	6.92(6.73)	Los of coordinated water molecules ($2H_2O$)	[Cu(HL)Cl]
	170-230	6.45 (6.62)	Loss of chloride ions (Cl)	[Cu(HL)]
	230-532	69.77 (71.80)	Decomposition of the complex forming CuO	CuO
(4)	270-310	11.77(12.07)	Loss of two acetate ions ($2CH_3COOH$)	$[Cu(H_2L)_2]$
	320-620	79.20 (79.85)	Decomposition of the complex forming CuO	CuO
(5)	145-220	33.50(33.64)	Los of three coordinated water molecules and $C_8H_{10}N_2$	$[Cu(L\text{-}C_8H_{10}N_2)]$
	220-430	51.89(52.02)	Decomposition of the complex forming CuO	CuO
(9)	175-225	5.96 (6.50)	Los of coordinated water molecules ($2H_2O$)	[Ni(HL)(OAc)]
	230-330	17.00(16.17)	Loss of acetate ions (CH_3COOH) and $2CH_3$	$[Ni(HL\text{-}2CH_3)]$
	330-445	63.01(63.89)	Decomposition of the complex forming NiO	NiO
(10)	95-145	6.34 (6.84)	Los of coordinated water molecules ($2H_2O$)	[Fe(L)Cl]
	160-190	6.51 (6.73)	Loss of chloride ions (HCl)	[Fe(L)]
	220-600	69.00(71.27)	Decomposition of the complex forming Fe_2O_3	Fe_2O_3
(11)	22-80	6.06(5.75)	Dehydration process ($2H_2O$)	$[Ru(HL)Cl_2(H_2O)]$
	80-120	2.61(2.88)	Los of coordinated water molecules (H_2O)	$[Ru(HL)Cl_2]$
	120-245	11.30 (11.33)	Loss of chloride ions (2HCl)	[Ru(HL)]
	250-690	60.00 (60.07)	Decomposition of the complex forming Ru_2O_3	Ru_2O_3

***Table* 3.** Biological activities of the ligand and its metal complexes against bacteria and fungus

Compounds	Inhibition zone (IZ/mm)/Activity index (AI/%)					
	A. niger		*E. coli*		*B. subtilis*	
	IZ(mm)	AI(%)	IZ(mm)	AI(%)	IZ(mm)	AI(%)
DMSO	0		0	0	0	0
Amphotericin B	17	100	--	--	--	--
Tetracycline	--		35	100%	38	100%
Ligand	10	59%	8	23%	0	0%
Complex **(2)**	11	65%	9	26%	16	42%
Complex **(3)**	12	71%	0	0%	8	21%
Complex **(4)**	10	59%	9	26%	14	37%
Complex **(5)**	0	0%	15	43%	18	45%
Complex **(6)**	11	65%	14	40%	15	39%
Complex **(7)**	13	76%	18	51%	13	34%
Complex **(8)**	10	59%	8	23%	0	0%
Complex **(9)**	12	71%	14	40%	15	39%
Complex **(10)**	14	82%	17	49%	18	47%
Complex **(11)**	12	71%	10	29%	15	39%

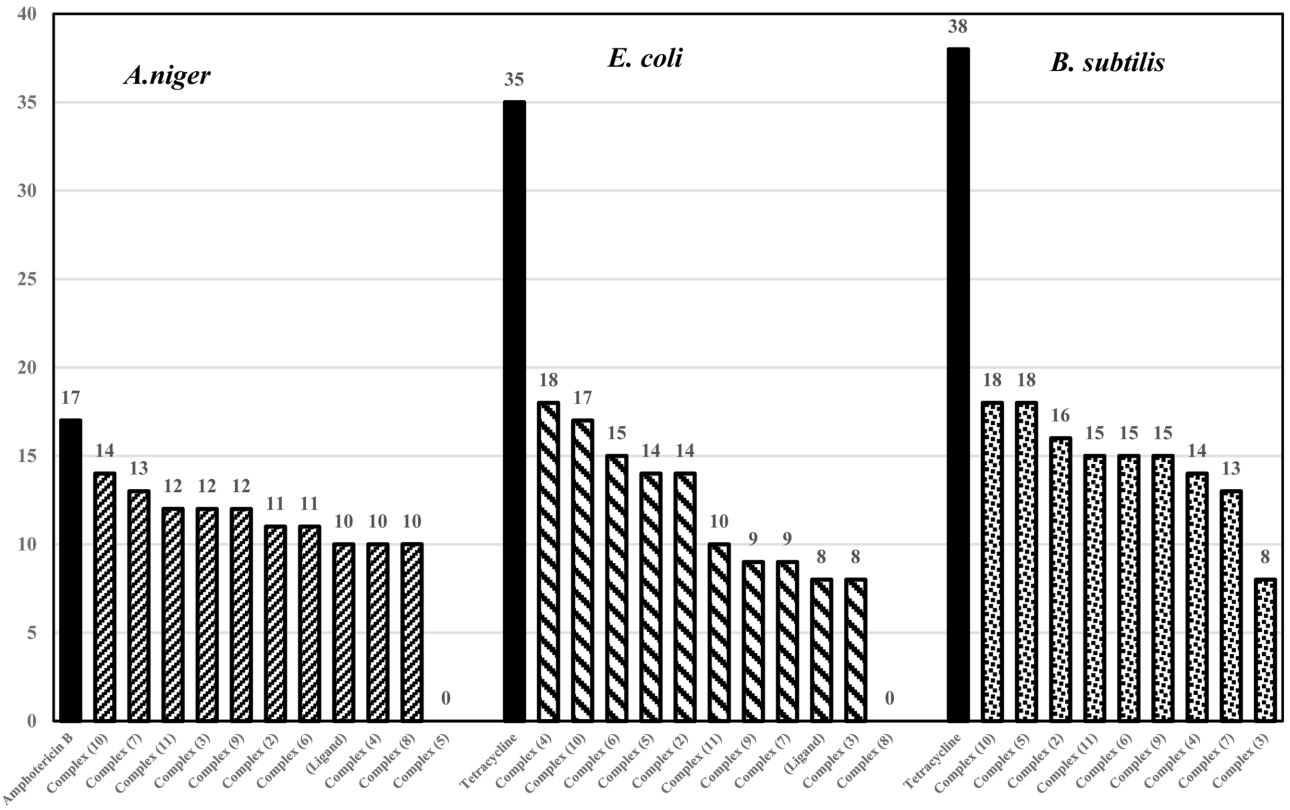

***Figure* 4.** Antimicrobial activities of ligand and its complexes against *A. flavus, C. albicans, E. coli* and *S. aureus.*

B. subtilis, the ligand and complex **(8)** are inactive, while the other complexes showed low activity in comparison with Tetracycline as an antibacterial standard drug. The antibacterial activity order against *B. subtilis* is **(5)=(10)>(2)>(6)=(9)=(11)>(4)>(7)>(3)** as shown in *Fig.* 4. The variation in the activity of different complexes against different microorganisms depend either on the impermeability of the microbial cells or differences in the ribosomes of microbial cells. The increased activity of the metal complexes can be explained based on Overtone's and Tweedy's theories. It

is known that coordination tends to make the coordinated ligand act as more powerful and potent bacterial and fungicidal agent, thus killing more of the bacteria and fungi than the free ligand precursor. It is observed that in a complex, the positive charge of the metal is partially shared with the donor atoms present in the ligand and there may be π-electron delocalization over the whole chelate. This increases the lipophilic character of the metal chelate and favors its permeation through the lipoid layer of the organism membrane. There are other factors which also increase the activity, which are the number of coordination sites, size of complex, solubility, conductivity and the bond lengths between the metal and the coordinated ligand atom.[62]

CONCLUSION

Cu(II), Ni(II), Co(II), Mn(II), Zn(II), Fe(III), Ru(III), and UO_2(II) complexes of a azo-hydrazone ligand, 2-hydroxy-4-(*p*-tolyldiazenyl) benzylidene)-2-(*p*-tolylamino) acetohydrazide **(H_2L)** were synthesized by a direct method. The new synthesized compounds were characterized by elemental and thermal analyses IR, NMR, and electronic absorption spectra as well as molar conductivity, magnetic moment. The data of various analyses revealed that the ligand chelated to the metal ions as a neutral/monobasic bidentate, monobasic/dibasic tridentate fashion through azomethine nitrogen, protonated/deprotonated phenolic hydroxyl group and/or ketonic/enolic carbonyl group Forming distorted octahedral or octahedral geometry around the centre metal ions. The thermal analysis confirmed that complexes **(2)**, **(4-5)** and **(9-11)** were decomposed in two, three or four stages starting with dehydration process, removal of coordination water molecules and/or elimination of anions and ended with complete degradation of the complexes with the formation metal oxide. The antimicrobial activity of prepared compounds *E. coli*, *B. subtilis* and *A. sniger* showed that these compounds exhibit a low activity in comparing with standard antifungal and antibacterial drugs.

Acknowledgments. Publication cost of this paper was supported by the Korean Chemical Society.

REFERENCES

1. Fischer, E., Verbindungen des Phenylhydrazins mit den Zuckerarten. **1884**, *17*, 579.
2. (a) Barakat, A.; Soliman, S. M.; Ali, M.; Elmarghany, A.; Al-Majid, A. M.; Yousuf, S.; Ul-Haq, Z.; Choudhary, M. I.; El-Faham, A. *Inorg. Chim. Acta* **2020**, *503*, 119405; (b) Li, Y.; Li, Y.; Liu, X.; Yang, Y.; Lin, D.; Gao, Q. *J. Mol. Struct.* **2020,** *1202*, 127229; (c) Bingul, M.; Ercan, S.; Boga, M. *J. Mol. Struct.* **2020**, *1213*, 128202; (d) Ramya Rajan, M. P.; Rathikha, R.; Nithyabalaji, R.; Sribalan, R. *J. Mol. Struct.* **2020,** *1216*, 128297.
3. Saouli, S.; Selatnia, I.; Zouchoune, B.; Sid, A.; Zendaoui, S. M.; Bensouici, C.; Bendeif, E.-E. *J. Mol. Struct.* **2020,** *1213*, 128203.
4. Dkhar, L.; Banothu, V.; Kaminsky, W.; Kollipara, M. R. *J. Organomet. Chem.* **2020**, *914*, 121225.
5. Szklarzewicz, J.; Jurowska, A.; Matoga, D.; Kruczała, K.; Kazek, G.; Mordyl, B.; Sapa, J.; Papież, M. *Polyhedron* **2020**, *185*, 114589.
6. Sreepriya, R. S.; Kumar, S. S.; V, S.; S, B.; Meena, S. S. *J. Mol. Struct.* **2020**, *1201*, 127110.
7. El-Barasi, N. M.; Miloud, M. M.; El-ajaily, M. M.; Mohapatra, R. K.; Sarangi, A. K.; Das, D.; Mahal, A.; Parhi, P. K.; Pintilie, L.; Barik, S. R.; Amin Bitu, M. N.; Kudrat-E-Zahan, M.; Tabassum, Z.; Al-Resayes, S. I.; Azam, M. *J. Saudi Chem. Soc.* **2020**, *24*, 492.
8. Çınarlı, M.; Yüksektepe Ataol, Ç.; Çınarlı, E.; İdil, Ö. *J. Mol. Struct.* **2020**, *1213*, 128152.
9. Chimmalagi, G. H.; Kendur, U.; Patil, S. M.; Gudasi, K. B.; Frampton, C. S.; Budri, M. B.; Mangannavar, C. V.; Muchchandi, I. S. *Appl. Organomet. Chem.* **2018**, *32*, e4337.
10. Hegde, Ganesh S.; Sandeep P. Netalkar.; and Vidyanand K. Revankar. *Applied Organometallic Chemistry*, **2019**, *33*, e4840.
11. Dehestani, L.; Ahangar, N.; Hashemi, S. M.; Irannejad, H.; Honarchian Masihi, P.; Shakiba, A.; Emami, S. *Bioorg. Chem.* **2018**, *78*, 119.
12. Heydari, R.; Motieiyan, E.; Aliabadi, A.; Abdolmaleki, S.; Ghadermazi, M.; Yarmohammadi, N. *Polyhedron* **2020**, *181*, 114477.
13. Patel, A. K.; Jadeja, R. N.; Roy, H.; Patel, R. N.; Patel, S. K.; Butcher, R. J.; Cortijo, M.; Herrero, S. *Polyhedron* **2020**, *186*, 114624.
14. Popiołek, Ł.; Patrejko, P.; Gawrońska-Grzywacz, M.; Biernasiuk, A.; Berecka-Rycerz, A.; Natorska-Chomicka, D.; Piątkowska-Chmiel, I.; Gumieniczek, A.; Dudka, J.; Wujec, M. *Biomedicine & Pharmacotherapy* **2020**, *130*, 110526.
15. Benkhaya, S.; M'Rabet, S.; El Harfi, A. *Inorg. Chem. Commun.* **2020**, *115*, 107891.
16. Aljamali, N. M.; Habeab, A. A.; Alfatlawi, I. O. *Int. J. Chem-inf. Res.* **2019**, *5*, 41.
17. Benkhaya, S.; M'Rabet, S.; El Harfi, A. *Heliyon* **2020**, *6*, e03271.
18. (a) Aamoum, A.; Waszkowska, K.; Taboukhat, S.; Płóciennik, P.; Bakasse, M.; Boughaleb, Y.; Strzelecki, J.; Korcala, A.; Sofiani, Z.; Zawadzka, A. *Optical and Quantum Electronics* **2019**, *52*, 35; (b) Abdel-Rahman, L. H.; Abu-Dief, A. M.; Moustafa, H.; Abdel-Mawgoud, A. A. H. *Arab. J. Chem.* **2020**, *13*, 649.
19. Ghanavatkar, C. W.; Mishra, V. R.; Sekar, N. *Spectrochim. Acta Part A Mol. Biomol. Spectrosc.* **2020**, *230*, 118064.
20. Mallikarjuna, N. M.; Keshavayya, J.; Prasanna, B. M.;

Praveen, B. M.; Tandon, H. C. *J. Bio- and Tribo-Corrosion* **2019**, *6*, 9.
21. (a) Alhakimi, A. N. *Egypt. J. Chem.* **2020**, *63*, 1509; (b) Aly, S. A.; Fathalla, S. K. *Arab. J. Chem.* **2020**, *13*, 3735.
22. (a) Patel, A. K.; Jadeja, R. N.; Butcher, R. J.; Kesharwani, M. K.; Kästner, J.; Muddassir, M. *Polyhedron* **2021**, *195*, 114969; (b) Abu-Dief, A. M.; El-Metwaly, N. M.; Alzahrani, S. O.; Bawazeer, A. M.; Shaaban, S.; Adam, M. S. S. *J. Mol. Liquids* **2021**, *322*, 114977; (c) Mohamad, A. D. M.; Abualreish, M. J. A.; Abu-Dief, A. M. *J. Mol. Liquids* **2019**, *290*, 111162.
23. Traven, V. F.; Cheptsov, D. A.; Mamirgova, Z. Z.; Solovjova, N. P.; Martynenko, V. M.; Dolotov, S. M.; Krayushkin, M. M.; Ivanov, I. V. *J. Photochem. Photobiol. B Biol.* **2020**, *n/a*.
24. (a) Said, M. A.; Al-unizi, A.; Al-Mamary, M.; Alzahrani, S.; Lentz, D. *Inorg. Chim. Acta* **2020**, *505*, 119434; (b) Almáši, M.; Vilková, M.; Bednarčík, J. *Inorg. Chim. Acta* **2021**, *515*, 120064; (c) Bera, P.; Aher, A.; Brandao, P.; Manna, S. K.; Bhattacharyya, I.; Pramanik, C.; Mandal, B.; Das, S.; Bera, P. *J. Mol. Struct.* **2021**, *1224*, 129015; (d) Fathi, A. M.; Mandour, H. S.; HassaneAnouar, E. *J. Mol. Struct.* **2021**, *1224*, 129263; (e) Sun, Y.; Lu, Y.; Bian, M.; Yang, Z.; Ma, X.; Liu, W. *Eur. J. Med. Chem.* **2021**, *211*, 113098.
25. Lawrence, M. A. W.; Lorraine, S. C.; Wilson, K.-A.; Wilson, K. *Polyhedron* **2019**, *173*, 114111.
26. (a) Liu, J. N.; Wu, B. W.; Zhang, B.; Liu, Y. *Turk. J. Chem.* **2006**, *30*, 41; (b) Shakdofa, M. M. E.; El-Saied, F. A.; Al-Hakimi, A. N. *Main Group Chem.* **2012**, *11*, 189.
27. (a) Jeffery, G. H.; Bassett, J.; Mendham, J.; Denney, R. C., *Vogel's Textbook of Quantitative Chemical Analysis*. 5th ed.; John Wiley & Sons Inc: 1989; (b) Svehla, G., *Vogel's textbook of macro and semi micro Quantitative inorganic analysis*. 5th ed.; Longman Inc.: New York, 1979; p 617.
28. Shakdofa, M. M. E.; El-Saied, F. A.; Rasras, A. J.; Al-Hakimi, A. N. *Appl. Organomet. Chem.* **2018**, *32*, e4376.
29. Lewis, L.; Wilkins, R. G., *Modern Coordination Chemistry*. Interscience: New York, 1960.
30. Boggess, R. K.; Zatko, D. A. *J. Chem. Educ.* **1975**, *52*, 649.
31. (a) Collee, J. G.; Mackie, T. J.; McCartney, J. E., *Mackie & McCartney practical medical microbiology*. 14 ed ed.; Churchill Livingstone: New York, 1996; p 978; (b) Holder, I. A.; Boyce, S. T. *Burns* **1994**, *20*, 426.
32. Zaky, R. R.; Ibrahim, K. M.; Gabr, I. M. *Spectrochim. Acta Part A Mol. Biomol. Spectrosc.* **2011**, *81*, 28.
33. Geary, W. J. *Coord. Chem. Rev.* **1971**, *7*, 81.
34. (a) Al-Ne'aimi, M. M.; Al-Khuder, M. M. *Spectrochim. Acta Part A Mol. Biomol. Spectrosc.* **2013**, *105*, 365; (b) Gup, R.; Kirkan, B. *Spectrochim. Acta Part A Mol. Biomol. Spectrosc.* **2005**, *62*, 1188; (c) Maurya, M. R.; Khurana, S.; Schulzke, C.; Rehder, D. *Eur. J. Inorg. Chem.* **2001**, 779.
35. Bessy Raj, B. N.; Prathapachandra Kurup, M. R.; Suresh, E. *Spectrochim. Acta Part A Mol. Biomol. Spectrosc.* **2008**, *71*, 1253.
36. (a) Hosseini Monfared, H.; Kheirabadi, S.; Asghari Lalami, N.; Mayer, P. *Polyhedron* **2011**, *30*, 1375; (b) Bayoumi, A. H.; Alaghaz, M. A. A. N.; Aljahdali, M. S. *Int. J. Electrochem. Sci.* **2013**, *8*, 9399.
37. Azam, M.; Al-Resayes, S. I.; Pallepogu, R.; Firdaus, F.; Shakir, M. *J. Saudi Chem. Soc.* **2016**, *20*, 120.
38. (a) Kurtoğlu, M.; Ispir, E.; Kurtoğlu, N.; Serin, S. *Dyes Pigm.* **2008**, *77*, 75; (b) Aly, S. A.; Fathalla, S. K. *Arab. J. Chem.* **2020**.
39. Mohamad M. E. Shakdofa; El-tabl, A. S.; Al-hakimi, A. S.; Wahba, M. A.; Morsy, N. *Ponte* **2017**, *73*, 52.
40. Han, H. O.; Kim, S. H.; Kim, K. H.; Hur, G. C.; Joo Yim, H.; Chung, H. K.; Ho Woo, S.; Dong Koo, K.; Lee, C. S.; Sung Koh, J.; Tae Kim, G. *Bioorg. Med. Chem. Lett.* **2007**, *17*, 937.
41. Andrew, F. P.; Ajibade, P. A. *J. Mol. Struct.* **2018**, *1170*, 24.
42. Xu, G. C.; Zhang, L.; Liu, L.; Liu, G. F.; Jia, D. Z. *Polyhedron* **2008**, *27*, 12.
43. Samanta, B.; Chakraborty, J.; Shit, S.; Batten, S. R.; Jensen, P.; Masuda, J. D.; Mitra, S. *Inorg. Chim. Acta* **2007**, *360*, 2471.
44. Bhosale, J. D.; Shirolkar, A. R.; Pete, U. D.; Zade, C. M.; Mahajan, D. P.; Hadole, C. D.; Pawar, S. D.; Patil, U. D.; Dabur, R.; Bendre, R. S. *J. Pharm. Res.* **2013**, *7*, 582.
45. Singh, B.; Srivastava, P. *Transition Met. Chem.* **1987**, *12*, 475.
46. El-Wahab, Z. H. A.; Mashaly, M. M.; Salman, A. A.; El-Shetary, B. A.; Faheim, A. A. *Spectrochim. Acta Part A Mol. Biomol. Spectrosc.* **2004**, *60*, 2861.
47. (a) Chandra, S.; Gupta, L. K. *Spectrochim. Acta Part A Mol. Biomol. Spectrosc.* **2005**, *61*, 1181; (b) Nakamoto, K., *Infrared and Raman Spectra of Inorganic and Coordination Compounds, Part B*, 6th ed.; John Wiley & Sons INC: USA, 2009; (c) El-Tabl, A. S.; Shakdofa, M. M. E.; Shakdofa, A. M. E., *J. Serb. Chem. Soc.* **2013**, *78*, 39.
48. Gupta, L. K.; Bansal, U.; Chandra, S. *Spectrochim. Acta Part A Mol. Biomol. Spectrosc.* **2007**, *66*, 972.
49. El-Dissouky, A.; Fahmy, A.; Amer, A. *Inorg. Chim. Acta* **1987**, *133*, 311.
50. Fouda, M. F. R.; Abd-Elzaher, M. M.; Shakdofa, M. M.; El-Saied, F. A.; Ayad, M. I.; El Tabl, A. S. *J. Coord. Chem.* **2008**, *61*, 1983.
51. (a) Al-Hakimi, A. N.; Shakdofa, M. M. E.; El-Seidy, A. M. A.; El-Tabl, A. S. *J. Korean Chem. Soc.* **2011**, *55*, 418; (b) Al-Hazmi, G. A. A.; Metwally, N. E. *Arab. J. Chem.* **2017**, *10*, S1003.
52. Shakdofa, M. M.; Al-Hakimi, A. N.; Elsaied, F. A.; Alasbahi, S. O.; Alkwlini, A. M. *Bull. Chem. Soc. Ethiop.* **2017**, *31*, 75.
53. Rageh, N. M.; Mawgoud, A. M. A.; Mostafa, H. M. *Chem. Pap.* **1999**, *53*, 107.
54. Gup, R.; Giziroglu, E.; Kirkan, B. *Dyes Pigm.* **2007**, *73*,

40.
55. (a) El-Tabl, A. S.; Aly, F. A.; Shakdofa, M. M. E.; Shakdofa, A. M. E. *J. Coord. Chem.* **2010**, *63*, 700; (b) Lever, A. B. P., *Inorganic electronic spectroscopy.* Elsevier science: Amsterdam 1984.
56. El-Tabl, A. S.; Shakdofa, M. M. E.; Labib, A. A.; Al-Hakimi, A. N. *Main Group Chem.* **2012**, *11*, 311.
57. Krishnapriya, K. R.; Kandaswamy, M. *Polyhedron* **2005**, *24*, 113.
58. (a) El-Tabl, A. S.; El-Enein, S. A. *J. Coord. Chem.* **2004**, *57*, 281; (b) Graham, B.; Spiccia, L.; Skelton, B. W.; White, A. H.; Hockless, D. C. R. *Inorg. Chim. Acta* **2005**, *358*, 3974.
59. Tiliakos, M.; Cordopatis, P.; Terzis, A.; P. Raptopoulou, C.; Perlepes, S. P.; Manessi-Zoupa, E. *Polyhedron* **2001**, *20*, 2203.
60. (a) Venkatachalam, G.; Ramesh, R. *Spectrochim. Acta Part A Mol. Biomol. Spectrosc.* **2005**, *61*, 2081; (b) Viswanathamurthi, P.; Dharmaraj, N.; Anuradha, S.; Natarajan, K. *Transition Met. Chem.* **1998**, *23*, 337; (c) Karvembu, R.; Jayabalakrishnan, C.; Natarajan, K. *Transition Met. Chem.* **2002**, *27*, 574.
61. Gandhi, J. B.; Kulkarni, N. D. *Transition Met. Chem.* **2001**, *26*, 96.
62. (a) Creaven, B. S.; Duff, B.; Egan, D. A.; Kavanagh, K.; Rosair, G.; Thangella, V. R.; Walsh, M. *Inorg. Chim. Acta* **2010**, *363*, 4048; (b) Tümer, M.; Köksal, H.; Sener, M. K.; Serin, S. *Transition Met. Chem.* **1999**, *24*, 414; (c) Tweedy, B. G. *Phytopathology* **1964**, *55*, 910.